Defense Technical Information Center
Compilation Part Notice

ADP011165

TITLE: Adaptive Algorithms for Control of Combustion

DISTRIBUTION: Approved for public release, distribution unlimited

This paper is part of the following report:

TITLE: Active Control Technology for Enhanced Performance Operational
Capabilities of Military Aircraft, Land Vehicles and Sea Vehicles
[Technologies des systemes a commandes actives pour l'amelioration des
performances operationnelles des aeronefs militaires, des vehicules
terrestres et des vehicules maritimes]

To order the complete compilation report, use: ADA395700

The component part is provided here to allow users access to individually authored sections
of proceedings, annals, symposia, etc. However, the component should be considered within
the context of the overall compilation report and not as a stand-alone technical report.

The following component part numbers comprise the compilation report:
ADP011101 thru ADP011178

Adaptive Algorithms for Control of Combustion

S. Evesque
Engineering Department
Cambridge University
Trumpington Street
Cambridge CB2 1PZ, UK

A.P. Dowling
Engineering Department
Cambridge University
Trumpington Street
Cambridge CB2 1PZ, UK

A.M. Annaswamy
Dept of Mechanical Engineering
Massachusetts Institute of Technology
Room 3-461B – 77 Massachusetts Avenue
Cambridge MA 02139-4307, USA

Abstract

Rather than investigate a particular combustor, a whole class of combustion systems, susceptible to damage from combustion instabilities, is considered. Under some simple and realistic assumptions (pressure waves reflected from the combustor boundaries smaller than incoming waves, flame stable in itself, limited bandwith flame response), it is demonstrated that a finite dimensional approximation to the open-loop transfer function of such a combustion system satisfies some general properties (stable zeros, small relative degree) that are exploited to design adaptive active controllers guaranteed to stabilise the self-excited combustion oscillations. In particular, for the practical case of a combustion system with time delay, a completely new and simple adaptive control design is presented and a formal proof for stability is given. The performance of such stable adaptive controllers is illustrated in a simulation.

1. Introduction

In order to meet stringent emission requirements, combustors are increasingly being designed to operate in a lean premixed mode. Although this reduces the NOx emissions, it has the disadvantage that premixed flames are particularly susceptible to self-excited oscillations, and the associated large-scale pressure waves can cause structural damage. *Active* control provides a way of extending the stable operating range of a combustion system, by interrupting the damaging interaction between acoustic waves and unsteady combustion. However, to be useful in practice, an active controller needs to be effective across a range of operating conditions. An efficient approach is to use an *adaptive* controller in which the controller transfer function is continually altered as the engine condition changes.

They are already some algorithms that describe how to update the controller parameters. The most popular adaptive schemes used for active control of combustion instability is the Least Mean Squares (LMS) algorithm applied to an IIR (Infinite Impulse Response) filter [5],[17],[12],[11]. The LMS is very attractive because it does not require any theoretical model: the combustion process is considered as a 'black box' and is learnt during a system identification procedure, performed off-line [5] or on-line [17],[12],[11] thanks to measurements. However, the major drawback is that an LMS controller might lead to a divergence of the control scheme if, for some operating conditions, the poles of the IIR become unstable. The features of a LMS controller have been extensively studied by Evesque & Dowling [12],[11], and here it was necessary to introduce a parallel algorithm (based on the Laguerre's method [28]) to prevent a starting divergence due to the controller. Other adaptive schemes already developed include neural networks [6] which is a nonlinear version of the LMS-controller, and a minimisation scheme based on the downhill simplex algorithm [25]. All these schemes provide no guarantee that the controller can stabilise the self-excited combustion process.

An efficient way to prevent any divergence of the adaptive control scheme is to use systematic methods for designing stable adaptive systems. The adaptive controller, called STR (Self-Tuning Regulator) by Annaswamy et al [2], is designed based on a Lyapunov stability analysis and is therefore guaranteed to be stable for any operating conditions. Furthermore, the STR has the advantage of avoiding a system identification procedure (which is one of the main difficulties in implementing a LMS controller [12]), since it uses little information about the physical process. However, so far, only a specific simple combustor has been shown to have the structure required for the design of a STR [2]. Moreover, the STR cannot accommodate a time delay between control action and its detection.

Our purpose in this paper is to:
(i) determine the general features of a self-excited combustion system, rather than investigate a particular combustor in detail.
(ii) exploit these features to design a novel adaptive controller that is guaranteed to stabilise the combustion system, the major challenge being to guarantee stabilisation in the presence of time delay in the combustion system.
Step (ii) involves first the choice of a low order fixed controller structure that can stabilise the system, and second the determination of adaptive laws for the controller parameters guaranteed to converge to stabilising values.

Hence, the paper is divided as follows: in section 2, a whole class of self-excited combustion systems is described, and its features used to build a controller are given. Section 3 describes low order fixed regulator structures that can control a combustion system with or without time delay, while section 4 deals with the design of a Self Tuning Regulator (STR) guaranteed to stabilise a self-excited combustion process, containing or not some time delays. In section 5, the performance of the STR is illustrated on a simulation based on a nonlinear model of a premixed ducted flame developed by Dowling [10].

2. General features of self-excited combustion systems

Most premixed combustors are highly resonant systems and may develop combustion instabilities for some operating conditions. These self-excited oscillations result from an interaction between unsteady combustion and acoustic waves: unsteady combustion generates sound, while acoustic waves reflected from the boundaries perturb the combustion still further. Rather than investigate a particular combustor in detail, we determine the general structure of this interaction, which will then be exploited to design fixed and adaptive controllers in sections 3 and 4 respectively.

2.1 Open-loop characteristics

A wide class of combustion systems, including lean premixed prevapourised (LPP) combustors and aeroengine afterburners, can be modelled as a combustion section embedded within a network of pipes, as shown in figure 1. We will investigate linear low frequency perturbations to the flow in such a pipework system. The flow at inlet to the combustor is assumed to be isentropic, and the frequencies of interest are low. This ensures that the combustion zone is short compared with the wavelength. Moreover, since only plane waves transport acoustic energy, it is sufficient to consider one-dimensional disturbances. The pressure and velocity upstream the flame can therefore be written as a linear combination of the waves g and f, and downstream the
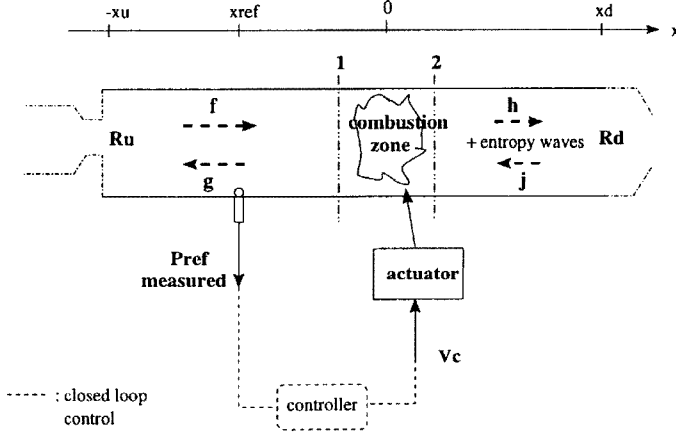
Figure 1: Open-loop self-excited combustion process with actuation

flame as a linear combination of the waves h and j:
in $-x_u < x < 0$,

$$
\begin{aligned}
p(x,t) &= \bar{p}_1 + f\left(t - \frac{x}{\bar{c}_1 + \bar{u}_1}\right) + g\left(t + \frac{x}{\bar{c}_1 - \bar{u}_1}\right) \\
u(x,t) &= \bar{u}_1 + \frac{1}{\bar{\rho}_1 \bar{c}_1}\left[f\left(t - \frac{x}{\bar{c}_1 + \bar{u}_1}\right) - g\left(t + \frac{x}{\bar{c}_1 - \bar{u}_1}\right)\right]
\end{aligned} \quad (1)
$$

in $0 < x < x_d$,

$$
\begin{aligned}
p(x,t) &= \bar{p}_2 + h\left(t - \frac{x}{\bar{c}_2 + \bar{u}_2}\right) + j\left(t + \frac{x}{\bar{c}_2 - \bar{u}_2}\right) \\
u(x,t) &= \bar{u}_2 + \frac{1}{\bar{\rho}_2 \bar{c}_2}\left[h\left(t - \frac{x}{\bar{c}_2 + \bar{u}_2}\right) - j\left(t + \frac{x}{\bar{c}_2 - \bar{u}_2}\right)\right]
\end{aligned} \quad (2)
$$

p, u, ρ and c are respectively the pressure, velocity, density and speed of sound. The suffices 1 and 2 denote flow quantities just upstream and downstream of the combustion zone, and the over-bar indicates a mean value. The distances x_u and x_d are the lengths upstream and downstream of the combustion zone.

The boundary conditions of the combustor are characterized by upstream and downstream pressure reflection coefficients R_u and R_d respectively. Since this boundary condition neglects the conversion of combustion-generated entropy waves into sound at any downstream nozzle, we expect it to be a good approximation when the time taken for entropy waves to convect through the straight duct, $\bar{u}_2/x_d$, exceeds their diffusion time. We consider linear disturbances with time dependence e^{st}, and assume that in the half plane $Real(s) \geq 0$:

$$
\begin{aligned}
|R_u(s)| &< 1, \\
|R_d(s)| &< 1.
\end{aligned} \quad (3)
$$

Physically, this means that the amplitude of the reflected wave is less than the incoming wave and may include some time delay. Simple duct terminations like open and choked ends trivially satisfy this condition, provided appropriate energy loss mechanisms are included. In appendix A, we show that condition (3) is also satisfied by reflection from general pipework configurations with negligible mean flow. The reflected waves f and j are easily obtained from g and h using the combustor boundary conditions*:

$$
\begin{aligned}
f(t) &= R_u(s)[g(t - \tau_u)] \quad at \quad x = -x_u \\
j(t) &= R_d(s)[h(t - \tau_d)] \quad at \quad x = x_d,
\end{aligned} \quad (4)
$$

where $\tau_u = 2x_u/\bar{c}_1(1 - \bar{M}_1^2)$ and $\tau_d = 2x_d/\bar{c}_2(1 - \bar{M}_2^2)$ are respectively the upstream and downstream propagation time delays, and $\bar{M}$ is the mean flow Mach number.

---

*$F(s)[\ ]$ is an operator of the variable $s = \frac{d}{dt}$. For instance, $x(t) = \frac{1}{s+1}[y(t)]$ means that $\frac{dx}{dt}(t) + x(t) = y(t)$.

The equations of conservation of mass, momentum and energy across the short flame zone at $x = 0$ can be written in a form that is independent of downstream density and temperature [9]:

$$
\begin{aligned}
p_2 - p_1 + \rho_1 u_1(u_2 - u_1) &= 0 \\
\frac{\gamma}{\gamma - 1}(p_2 u_2 - p_1 u_1) + \frac{1}{2}\rho_1 u_1(u_2^2 - u_1^2) &= \frac{Q}{A}.
\end{aligned} \quad (5)
$$

Q is the instantaneous rate of heat release, A is the combustor cross-sectional area and γ is the ratio of specific heat capacities. Substitution from (1), (2) and (4) into (5), making use of the isentropic condition p_1/ρ_1^γ, and linearising in the flow perturbations give the time evolution of the outgoing waves g and h generated by the unsteady heat release $Q(t)$:

$$
\begin{pmatrix} X_{11} & X_{12} \\ X_{21} & X_{22} \end{pmatrix} \begin{pmatrix} g(t) \\ h(t) \end{pmatrix} = \begin{pmatrix} Y_{11}R_u & Y_{12}R_d \\ Y_{21}R_u & Y_{22}R_d \end{pmatrix} \begin{pmatrix} [g(t - \tau_u)] \\ [h(t - \tau_d)] \end{pmatrix}
$$
$$
+ \begin{pmatrix} 0 \\ \frac{Q(t) - \bar{Q}}{A\bar{c}_1} \end{pmatrix} \quad (6)
$$

where X_{ij} and Y_{ij} are constant coefficients depending on the mean flow only, and given in appendix B.

After taking the Laplace transform[†] of the system (6) and using (1) and the boundary condition (4), one obtains the transfer function

$$
G(s) = \frac{u_1(s)}{Q(s)} = \frac{(R_d Y_{12}e^{-s\tau_d} - X_{12})(R_u e^{-s\tau_u} - 1)}{\det(N)} \quad (7)
$$

where

$$
N = \begin{pmatrix} X_{11} - R_u Y_{11}e^{-s\tau_u} & X_{12} - R_d Y_{12}e^{-s\tau_d} \\ X_{21} - R_u Y_{21}e^{-s\tau_u} & X_{22} - R_d Y_{22}e^{-s\tau_d} \end{pmatrix}.
$$

$G(s)$ describes the generation of unsteady velocity $u_1(t)$ at the flame, due to the unsteady heat release $Q(t)$.

Since the self-excited oscillation results from a coupling between unsteady heat release and acoustic waves, the forcing of unsteady heat release due to incoming flow disturbances at the flame must be also described. In many applications, the combustion responds most strongly to velocity fluctuations. This is because in acoustic waves the fractional change in flow velocity is order $\bar{M}^{-1}$ larger than the fractional change in pressure, ie a large factor at the low Mach numbers at which combustion can be sustained. This dependence on flow velocity can either be seen directly through its influence on flame kinematics and shape [10],[13], or indirectly through its influence on fuel-air ratio and hence on the rate of combustion in LPP systems [29]. A transfer function

$$
H(s) = \frac{Q(s)}{u_1(s)} \quad (8)
$$

is introduced to describe this combustion response. In many circumstances, $H(s)$ will include substantial time delays. Models for the flame transfer function $H(s)$ have been published in the literature for different combustors. However, we do not want to restrict our controller design to any particular combustion system or model. Instead we will make general, non-restrictive observations about the structure of the transfer function $H(s)$:

- (I) The flame is stable when there is no driving velocity u, which means that the poles of $H(s)$ are 'stable' (ie, are in the half plane $Real(s) < 0$ and so lead to eigenmodes with negative growth rate).

- (II) The flame response has a limited bandwith, therefore $H \to 0$ when $s \to \infty$.

These assumptions about $H(s)$ fit many flame models given in the literature, including premixed flames [10] and LPP systems [14]. The eigenfrequencies can be determined by combining equations (7) and (8). They satisfy

---

[†]The same notation is used for a temporal signal and its Laplace transform, for instance $u(t)$ and $u(s)$.

$$1 - G(s)H(s) = 0. \tag{9}$$

When a combustor is unstable, there are roots of equation (9) with $Real(s) > 0$: linear perturbations grow exponentially in time. We will design a feedback controller to stabilise such a system.

2.2 Actuated combustion system

In order to apply active control to our self-excited combustion system, an actuator is used to inject a perturbation and hence break the damaging coupling between unsteady combustion and acoustic waves. The two most commonly used active control inputs are loudspeaker forcing and fuel-forcing ([18] [26][4]). We will concentrate on fuel forcing which is the most relevant for practical applications. An actuator is driven to provide extra fuel (and sometimes air) which in turn produces additional heat release. In order to describe the impact of this input on the combustion system characteristics, we study the relationship between V_c, a voltage sent to the actuator, and P_{ref}, the fluctuating pressure measured at a location x_{ref} (see figure 1). That is, our goal is to characterize the transfer function

$$W(s) = \frac{P_{ref}(s)}{V_c(s)}, \tag{10}$$

which represents the actuated open-loop combustion process. We derive this transfer function in the following.

We assume that the fuel injection is arranged so that the external voltage V_c results in the additional heat release Q_c through the following transfer function

$$\frac{Q_c(s)}{V_c(s)} = W_a(s)e^{-s\tau_a}, \tag{11}$$

where $W_a(s)$ represents the actuator dynamics. Typically the actuator will be a valve with the characteristics of a mass-spring-damper system, whose dynamics are described by the transfer function $W_a(s)$. If the fuel-air mixture is injected directly into the combustion zone, the combustion response will be instantaneous ($\tau_a = 0$). However, if only fuel is added, there will be a small mixing time delay before it is burnt ($\tau_a > 0$). Often it is hazardous to inject fuel directly into the flame. If the additional fuel is introduced some distance upstream of the combustion zone, there will be a convection time delay τ_a between injection and combustion. In a LPP system, it is convenient to modulate the main fuel supplied in the premix ducts, in which case τ_a may be a significant proportion of the period of the self-excited oscillations. Notice that τ_a is independent of the flame radial position, which means that we assume the same time delay between all fuel injection and its combustion. When the combustion zone is short this is trivially satisfied. If the combustion zone is extensive, it may be necessary just to inject fuel in a localised region to meet this constraint.

There will be additional unsteady heat release driven by the flow fluctuations. We will denote this naturally occuring rate of heat release by Q_n. It is related to the velocity fluctuations by the flame model in (8):

$$H(s) = \frac{Q_n(s)}{u_1(s)}. \tag{12}$$

For linear fluctuations, we can superimpose the fluctuating heat release due to external actuation Q_c and the naturally occuring heat release Q_n to give the total fluctuating rate of heat release:

$$Q(s) = Q_c(s) + Q_n(s). \tag{13}$$

The acoustic waves generated by $Q(s)$ are described by (7), ie

$$G(s) = \frac{u_1(s)}{Q(s)}. \tag{14}$$

From equations (11)-(13), one obtains that:

$$\frac{u_1(s)}{V_c(s)} = \frac{G(s)W_a(s)e^{-s\tau_a}}{1 - G(s)H(s)}. \tag{15}$$

If the unsteady pressure P_{ref} is measured upstream the flame ($x_{ref} < 0$), then P_{ref} is a linear combination of the upstream waves f and g. Using (1) and the boundary condition (4) at $x = -x_u$, one easily obtains:

$$\frac{P_{ref}(s)}{u_1(s)} = \bar{\rho}_1 \bar{c}_1 \frac{1 + R_u e^{\frac{-2s(x_u + x_{ref})}{\bar{c}_1(1 - \bar{M}_1^2)}}}{R_u e^{-s\tau_u} - 1} \cdot e^{\frac{s x_{ref}}{\bar{c}_1 - \bar{u}_1}} \tag{16}$$

Therefore, it follows from (15) and (16) that the open-loop transfer function of the actuated system given in (10) can be written in the form:

$$W(s) = \frac{P_{ref}(s)}{V_c(s)} = W_0(s)e^{-s\tau_{tot}}, \tag{17}$$

where

$$\tau_{tot} = \tau_{det} + \tau_a \tag{18}$$

is the total time delay in the actuated system, τ_a is the time delay due to the actuation, $\tau_{det} = -x_{ref}/(\bar{c}_1 - \bar{u}_1)$ is the detection time delay due to the pressure measurement location, and

$$W_0(s) = \bar{\rho}_1 \bar{c}_1 \cdot \frac{G(s)W_a(s)}{1 - G(s)H(s)} \cdot \frac{1 + R_u e^{\frac{-2s(x_u + x_{ref})}{\bar{c}_1(1 - \bar{M}_1^2)}}}{R_u e^{-s\tau_u} - 1}, \tag{19}$$

with $G(s)$ and $H(s)$ given in equations (7) and (8).

If P_{ref} is measured downstream the flame ($x_{ref} > 0$), then P_{ref} is a linear combination of the downstream waves h and j. A simple calculation, using the wave structure in equations (1) and (2) and the continuity condition across the combustion zone in equation (5)a, shows that the transfer function $P_{ref}(s)/V_c(s)$ again has the form given in (17), provided that the right-hand side of equation (19) is multiplied by

$$P_{du}(s) = \frac{-X_{11} + R_u Y_{11}e^{-s\tau_u}}{X_{12} - R_d Y_{12}e^{-s\tau_D}} \frac{1 + R_d e^{-2s\frac{x_d - x_{ref}}{\bar{c}_2(1 - \bar{M}_2^2)}}}{1 + R_u e^{-2s\frac{x_u + x_{ref}}{\bar{c}_1(1 - \bar{M}_1^2)}}} e^{-s\left(\frac{x_{ref}}{\bar{c}_2 + \bar{u}_2} + \frac{x_{ref}}{\bar{c}_1 - \bar{u}_1}\right)} \tag{20}$$

2.3 General structural properties of the open-loop system useful for control design

For the sake of clarity, only the case of an upstream pressure measurement is considered here, but similar results can be derived for a downstream pressure measurement, using the expression of $P_{du}(s)$ given in (20). The wave description of linear perturbations in sections 2.1 and 2.2 gives the open-loop transfer function $W(s)$ in a particularly convenient form:

$$W(s) = e^{-s\tau_{tot}}W_0(s), \tag{21}$$

ie the product of a pure time delay and the transfer function $W_0(s)$ defined in (19). We will now show that $W_0(s)$ has some general structural properties that are useful for the control design. First $W_0(s)$ given in equation (19) is expanded into a rational form. This is achieved by applying the Padé approximation technique [3] for each exponential term of $W_0(s)$. This technique has been widely used in handling systems with time delays. We will use the notation $\left[\frac{L}{M}\right]_{f(s)}$ to denote the $(L, M)^{th}$ order Padé approximant of a function $f(s)$, which is a rational function $P(s)$ whose numerator has order L and denominator order M. The rational function $P(s)$ is chosen such that the first $L + M + 1$ terms in the power series of $P(s)$ will match those of $f(s)$, ie

$$f(s) = \left[\frac{L}{M}\right]_{f(s)} + O(s^{L+M+1}). \tag{22}$$

Lemma 1: *The zeros of W_0 are stable (ie are in $Real(s) < 0$): $W_0(s)$ is said to be 'minimum phase'*

Note that a rational approximation of the multiplying time delay $e^{-s\tau_{tot}}$ in equation (21) introduces unstable zeros into the open-loop transfer function $W(s) = W_0(s)e^{-s\tau_{tot}}$: it is $W_0(s)$ that is minimum phase, and not the overall transfer function $W(s)$. The time delays in the expression of $W_0(s)$ given in (19) are approximated by Padé expansions to give a rational approximation to the transfer function $W_0(s)$, and the stability of the zeros of $W_0(s)$ is discussed. First, it is evident from equation (19) that the poles of the flame transfer function $H(s)$ become zeros of $W_0(s)$. As noted in assumption (I), the condition that the flame is stable when there is no driving velocity u_1 ensures that these zeros are all in $Real(s) < 0$. Therefore $H(s)$ does not introduce unstable zeros for W_0. Secondly, $G(s)$ appears at the numerator and the denominator of $W_0(s)$, therefore its poles do not influence the zeros of $W_0(s)$. Thirdly, we assume that $W_a(s)$ has no unstable zeros. Fourthly, the numerator of W_0 includes $G(s)$ defined in (7) and is the product of terms of the form $K_1(s) + K_2(s)e^{-s\tau}$, where τ is a time delay, and $|K_1(s)/K_2(s)| > 1$ for $Real(s) \geq 0$ (because the reflection coefficients $R_u(s)$ and $R_d(s)$ have modulus strictly smaller than 1 for $Real(s) \geq 0$, and also because $X_{12} > |Y_{12}|$). These factors have no zeros in $Real(s) \geq 0$, because at a zero

$$e^{-s\tau} = -\frac{K_1(s)}{K_2(s)}. \tag{23}$$

Equation (23) cannot be satisfied in the half-plane $Real(s) \geq 0$, because there $|e^{-s\tau}| \leq 1$, while $|K_1(s)/K_2(s)| > 1$. We need to check that this remains true after a suitable Padé expansion of $e^{-s\tau}$. After the Padé approximation is made, one has to solve equations of the type

$$\left[\frac{L}{M}\right]_{e^{-s\tau}} = \frac{-K_1(s)}{K_2(s)}, \tag{24}$$

in order to find the remaining zeros of W_0. Baker & Graves-Morris [3] introduce the concept of A-acceptability for rational functions: a rational function $R(z)$ is A-acceptable if $|R(z)| < 1$ for $Real(z) < 0$. They go on to prove that the Padé approximant of the exponential function $[L/M]_{e^z}$ is A-acceptable provided that $M = L$, $L + 1$ or $L + 2$. Therefore, with such a choice of L and M, we obtain that

$$|[L/M]_{e^{-s\tau}}| < 1 \qquad for \qquad Real(-s\tau) < 0. \tag{25}$$

However, $|K_1(s)/K_2(s)| > 1$ for $Real(s) \geq 0$, so equation (24) has no roots in $Real(s) > 0$. On $Real(s) = 0$, the numerator and denominator of the Padé approximant $[L/M]_{e^{-s\tau}}$ are complex conjugate when $L = M$, which means that $|[M/M]_{e^{-s\tau}}| = 1$ in $Real(s) = 0$. Hence, since $|K_1(s)/K_2(s)| > 1$ for $Real(s) = 0$, equation (24) has no roots on $Real(s) = 0$, when $L = M$.

Therefore, it has been proved that all the zeros of W_0 are stable, provided that the $(L, M)^{th}$ order of each Padé approximant is chosen so that $M = L$, for any M.

Lemma 2: *The relative degree of W_0 is equal to the relative degree of the actuator transfer function*
An essential feature required for the control design is the relative degree n^* of W_0, denoted $n^*(W_0)$, which is the degree of the denominator of W_0 minus the degree of its numerator. $n^*(W_0)$ is the sum of the relative degrees of its various factors. Again working from the definition from the definition of W_0 in (19):

- $n^*(G(s)) = 0$ when the $(L, M)^{th}$ order Padé approximant for each exponential term $e^{-s\tau_u}$ and $e^{-s\tau_d}$ satisfies $L \leq M$ (we assume that $R_u(s)$ and $R_d(s)$ have a relative degree equal to zero, as it is described in Appendix A).

- similarly, $n^*\left(\frac{1 + R_u e^{\frac{-2s(x_u + x_{ref})}{\bar{c}_1(1 - \bar{M}_1^2)}}}{R_u e^{-s\tau_u} - 1}\right) = 0$ when the $(L, M)^{th}$ order Padé approximants for each exponential term $e^{-s\tau_u}$ and $e^{\frac{-2s(x_u + x_{ref})}{\bar{c}_1(1 - \bar{M}_1^2)}}$ satisfies $L \leq M$.

- $n^*(H) \geq 0$ since the flame has a limited bandwidth response (assumption (II)). Therefore, $H(s)$ does not affect the relative degree of W_0.

Finally, it appears that the relative degree of W_0 is equal to the relative degree of the actuator transfer function W_a, when each Padé approximant $[L/M]$ satisfies $L \leq M$.

Lemma 3: *The high frequency gain of W_0 is positive*
The controller design requires information on the sign of the high frequency gain k_0 of W_0 [21], defined as follows:

$$W_0(s) = k_0 \frac{Z_0(s)}{R_0(s)}, \tag{26}$$

where k_0 is a constant, and $Z_0(s)$ and $R_0(s)$ are two monic[‡] polynomials. To find $sign(k_0)$, we simply need to find equivalent expressions at large s for each factor of W_0. As noted in assumption (II), $H \to 0$ for $s \to \infty$. Furthermore, $n^*(G) = 0$, so that

$$1 - G(s)H(s) \sim 1 \qquad for \qquad s \to \infty. \tag{27}$$

The other factors of W_0 are terms of the form $1 + R(s)e^{-s\tau}$, where τ is a time delay. Make a Padé approximation: $e^{-s\tau} = [L/M]$, with $L = M$. Hence the high frequency gain of $[L/M]$ is $(-1)^M$. In appendix A is shown that the high frequency gain h of $R(s)$ satisfies $|h| < 1$. Therefore, the high frequency gain $1 + h(-1)^M$ of the term $1 + R(s)e^{-s\tau}$ has the same sign as 1. Finally, at high frequencies, the gain of W_0 is easily found to be positive when each Padé approximant $[L/M]$ satisfies $L = M$.

There is a straightforward reason why $W_0(s)$, in the open-loop transfer function $P_{ref}/V_c = W_0(s)e^{-s\tau_{tot}}$, has the simple properties outlined in lemmas 1 and 2. For $Real(s) \geq 0$, the amplitudes of the oscillations do not decrease with time and the boundary conditions $|R_u|, |R_d| < 1$ ensure that the largest contribution to P_{ref} is from the acoustic wave leaving the combustion zone, rather than the waves subsequently reflected from the boundaries. Under these circumstances, the main structure of $W_0(s)$ in equations (19) and (20) is dominated by the properties of $W_a(s)$, the other multiplying factors do not introduce unstable zeros nor affect the relative degree.

It is interesting to note that this argument remains true if the form of actuation is a loudspeaker, provided the loudspeaker is located within the combustion zone. However, this situation is more complicated when the loudspeaker is at a general axial position in the combustor. Then, since the combustion zone is an active component, it can reflect a wave of greater amplitude than the incident wave: if R_f denotes the reflection coefficient at the flame, $|R_f| > 1$ is possible even in $Real(s) \geq 0$ [27]. Under these circumstances, P_{ref}/V_c can have unstable zeros for some positions x_{ref}. Lemma 1 therefore is not true for general loudspeaker positions. This is consistent with the observations of Annaswamy et al [1] who calculated P_{ref}/V_c for a particular idealised combustor with loudspeaker actuation. They found that no simple relationship could be derived between the locations of the sensor, actuator and flame, and the zeros stability. For instance, for the particular case of sensor and actuator collocated at the flame, their open-loop plant P_{ref}/V_c had no unstable zeros. However, for the particular case of fuel forcing, the open-loop transfer function satisfies lemmas 1 and 2, properties that greatly help in the control design.

3. Fixed regulator design

We have shown that for fuel actuation the open-loop transfer function has a simple form: it can be written as the product of a pure time delay and a transfer function $W_0(s)$ which is rational after a Padé expansion is made: $P_{ref}(s)/V_c(s) = e^{-s\tau_{tot}}W_0(s)$. We will begin by designing a controller for the particular case

---

[‡]a monic polynomial denotes a polynomial whose leading coefficient is unity

$\tau_{tot} = 0$ and will then extend these ideas to the general and more practically relevant case $\tau_{tot} \neq 0$.

3.1 System without time delay ($\tau_{tot} = 0$)

It is clear from equation (18) that $\tau_{tot} = 0$ requires that the control fuel is injected and burnt with no time delay ($\tau_a = 0$), and that the reference pressure is measured in the combustion zone ($x_{ref} = 0$). Our open-loop combustion process is then described by

$$W_0(s) = \frac{P_{ref}(s)}{V_c(s)} = k_0 \frac{Z_0(s)}{R_0(s)} \qquad (28)$$

where k_0 is a positive constant, and Z_0 and R_0 are two monic polynomials. Furthermore, Z_0 and R_0 are 'coprime' polynomials, which means that they have no common factors. From lemma 1, we also know that Z_0 is a stable polynomial (ie it has only zeros in $Real(s) < 0$), whereas $R_0(s)$ has unstable zeros since our system exhibits self-excited oscillations. Finally, if R_0 has degree n, Z_0 has degree $n - n^*$, where

$$1 \leq n^* = n^*(W_a) \leq 2. \qquad (29)$$

($n^* = n^*(W_a)$ comes from lemma 2, and most practical actuators have a relative degree of 1 or 2).

To this open-loop system, we will apply an active feedback

$$\frac{V_c}{P_{ref}} = -K(s). \qquad (30)$$

The aim of the regulator is to stabilize the system, ie to make all the closed-loop poles stable. Combining (28) and (30) shows that these poles are the zeros of

$$R_{cl}(s) = R_0(s) + K(s)k_0 Z_0(s), \qquad (31)$$

The regulator transfer function $K(s)$ is to be determined using roots locus arguments [8]:

If $n^*(W_0) = 1$, consider the transfer function

$$K_1(s) = k_c, \qquad (32)$$

where k_c is a constant. Then the closed-loop poles are the zeros of the

$$R_{cl}(s) = R_0(s) + k_0 k_c Z_0(s). \qquad (33)$$

For $|k_c|$ 'large', $n - 1$ zeros of $R_{cl}(s)$ will be moved towards the $n - 1$ stable zeros of $k_0 Z_0(s)$. Investigation of the large $|s|$ asymptotic form shows that the nth zero of $R_{cl}(s)$ is also stabilised if $sign(k_c) = sign(k_0)$. Therefore, a finite value $k_{c_{min}} > 0$ exists such that

$$|k_c| > k_{c_{min}}, \quad sign(k_c) = sign(k_0) \qquad (34)$$

is a necessary and sufficient condition to stabilize our minimum phase plant of relative degree 1.

If $n^*(W_0) = 2$, and the regulator $K_1(s)$ is used, then a large $|k_c|$ will guarantee that $n - 2$ zeros of $R_{cl}(s)$ will be moved towards the stable zeros of $k_0 Z_0(s)$. The two remaining complex conjugate roots of $R_{cl}(s) = 0$ will be moved towards the stable half plane $Real(s) < 0$ only if

$$\begin{aligned} sign(k_c) &= sign(k_0) \\ \sum(zeros\,of\,R_0) - \sum(zeros\,of\,Z_0) &< 0. \end{aligned} \qquad (35)$$

As explained by Dorf & Bishop [8], equation (35)b guarantees that the asymptote centroid of the root locus is situated in the

left half plane $Real(s) < 0$. However, since (35) is not true in general, a better strategy is to use the following regulator:

$$K_2(s) = k_c \frac{s + z_c}{s + p_c}, \qquad (36)$$

where p_c and z_c are some positive constants, $p_c > z_c$. $K_2(s)$ corresponds to a phase-lead compensator, which adds phase, ie damping, in a frequency range $[z_c, p_c]$. Then the closed-loop poles are the zeros of

$$R_{cl}(s) = (s + p_c)R_0(s) + k_0 k_c(s + z_c)Z_0(s). \qquad (37)$$

For a 'large k_c' and an adequate choice of z_c and p_c, the n zeros of $R_{cl}(s)$ can be moved towards the left half plane. More precisely, a finite value $k_{c_{min}} > 0$ and some positive constants p_c and z_c exist such that

$$\begin{aligned} |k_c| &> k_{c_{min}} \\ sign(k_c) &= sign(k_0) \\ \sum(zeros\,of\,R_0) - \sum(zeros\,of\,Z_0) &< p_c - z_c \end{aligned} \qquad (38)$$

is a necessary and sufficient condition to stabilize a minimum phase plant of relative degree 2 with the regulator $K_2(s)$. Notice that $K_2(s)$ is also guaranteed to stabilize a minimum phase plant of relative degree 1.

In the following, the compensator $K_2(s)$ given in equation (36) will be implemented as shown in figure 2. The feedback transfer function for this system is given by

$$V_c = -\frac{k_2 V_c}{s + z_c} - k_1 P_{ref} \qquad (39)$$

ie

$$\frac{V_c}{P_{ref}} = -\frac{k_1(s + z_c)}{s + z_c + k_2}. \qquad (40)$$

It is clear from equations (40) and (36) that k_1 represents the gain k_c and k_2 determines the phase lag p_c in $K_2(s)$.
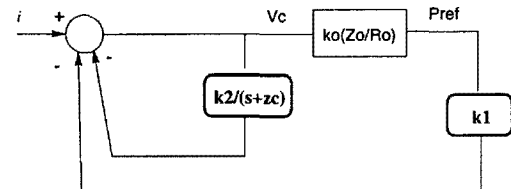

Figure 2: Fixed low-order controller structure for $\tau_{tot} = 0$, $n^* \leq 2$

However, the major drawback of such a fixed regulator $K_2(s)$ is that a cautious choice of p_c is necessary if the inequality (38)c is to be guaranteed without detailed knowledge of the plant. This in turn can mean that the gain k_c required to achieve control is large, especially to ensure stabilization under varying operating conditions, ie under uncertainties in the unstable frequencies ω_u. A large k_c means a large control effort, which is to be avoided. Therefore, to improve the response of our regulator $K_2(s)$ under varying operating conditions, one can choose a fixed $z_c > 0$, and make the other control parameters k_c and p_c adaptive. This is the topic of section 4 .

3.2 Combustion system with known time delay ($\tau_{tot} \neq 0$)

Here the combustion process is described by

$$W(s) = \frac{P_{ref}(s)}{V_c(s)} = k_0 \frac{Z_0(s)}{R_0(s)} e^{-s\tau_{tot}} = W_0(s)e^{-s\tau_{tot}}, \qquad (41)$$

with k_0 a constant, Z_0 and R_0 two coprime and monic polynomials, and τ_{tot} is a known time delay. R_0 has degree n, and Z_0

has degree $n - n^*$, with $n^* = 1$ or 2 (lemma 2). It was shown in section 2 that Z_0 is a stable polynomial (lemma 1) and that k_0 is positive (lemma 3).

In section 3.1, low order controllers of the form (32) and (36) were used to control the combustion process. Here, the presence of the time delay τ_{tot} makes such controllers inadequate, especially when τ_{tot} is of the order of the period of the unstable mode. Control of systems in the presence of time delays has been extensively studied [30][19][15]. A popular approach to accommodate large delays is due to O.J.M. Smith [30]. The Smith Controller (SC) attempts to estimate future outputs P_{ref} of the system using a known model, and provides an appropriate stabilization action. In Manitius & Olbrot [19], the SC was modified to control systems that are open-loop unstable by using finite-time integrals of inputs V_c to estimate future outputs (the goal of this modification was to avoid unstable pole-zero cancellations). In Ichikawa [15], a SC controller with finite-time integrals was derived to serve as a pole-placement controller. In [24] and [16], adaptive versions of the pole-placement controller have been developed and proved to be stable.

Since our plant is open-loop unstable, we want to implement a SC using the finite-time integral suggested by Manitius & Olbrot [19] and used in Ichikawa [15], and which is given by

$$V_{SC}(t) = \int_{-\tau_{tot}}^{0} \lambda(\sigma) V_c(t + \sigma) \, d\sigma, \qquad (42)$$

where $\lambda(\sigma)$ is a weighting function (it is shown in section 4.2 how discrete values of $\lambda(.)$ can be found by adaptation).

Briefly, the controller used in [15] and shown in figure 3 has the following form:

$$V_c(t) = -\frac{C(s)}{E(s)} [V_c(t - \tau_{tot})] - \frac{D(s)}{E(s)} [P_{ref}(t)] + \int_{-\tau_{tot}}^{0} \lambda(\sigma) V_c(t + \sigma) \, d\sigma \quad (43)$$

where the operators $C(s)$, $D(s)$ and $E(s)$ are chosen such that the denominator of the closed-loop transfer function matches a chosen stable polynomial. This can be achieved only if $degree(E) = n$, $degree(C) = n - 2$ and $degree(D) = n - 1$. This means that even for a plant of low relative degree ($n^* = 1$ or 2), if the order n is large, then the controller dynamics C/E and D/E will be of high order. This differs from the delay-free case described in section 3.1, for which a first order compensator could stabilize the plant of relative degree 2 or 1.
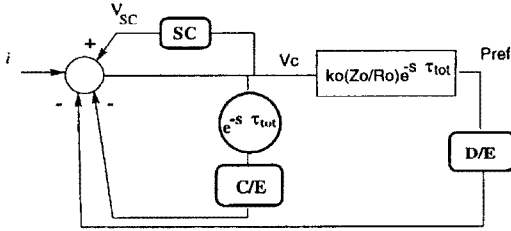

Figure 3: A nth order controller structure for $\tau_{tot} \neq 0$, given in Ichikawa's paper [15]

However, our aim is to keep a low order compensator to control the plant as it was done in section 3.1. Therefore, we suggest the controller structure given in figure 4. We begin as in [15] by choosing $\lambda(\sigma)$, the weighting function in the Smith Controller, to have the form

$$\lambda(\sigma) = \sum_{i=1}^{n} \alpha_i e^{-\beta_i \sigma}, \qquad (44)$$

where β_i are chosen to be the n zeros of the polynomial $R_0(s)$, whereas (at this stage) the α_i are arbitrary coefficients. Then, after substitution into (42) and evaluation of the integral, we obtain

$$V_{SC}(t) = \left(\frac{n_1(s)}{R_0(s)} - \frac{n_2(s)}{R_0(s)} e^{-s\tau_{tot}} \right) [V_c(t)], \qquad (45)$$

where

$$\frac{n_1(s)}{R_0(s)} = \sum_{i=1}^{n} \frac{\alpha_i}{s - \beta_i}$$

$$\frac{n_2(s)}{R_0(s)} = \sum_{i=1}^{n} \frac{\alpha_i}{s - \beta_i} e^{\beta_i \tau_{tot}} \qquad (46)$$

We prove in the following that the low order controller associated with the SC (see figure 4) will stabilize our minimum phase plant of relative degree 1 or 2 for a small τ_{tot}. With the controller structure described in figure 4, the closed-loop transfer function is given by

$$W_{cl}(s) = \frac{k_0(s + z_c) Z_0(s) e^{-s\tau_{tot}}}{R_{cl}(s)} = W_{cl_0}(s) e^{-s\tau_{tot}}, \qquad (47)$$

where the closed-loop poles are the zeros of

$$R_{cl}(s) = A(s) + B(s) e^{-s\tau_{tot}}, \qquad (48)$$

with

$$A(s) = (s + z_c)(R_0(s) - n_1(s)) + k_2 R_0(s) \qquad (49)$$

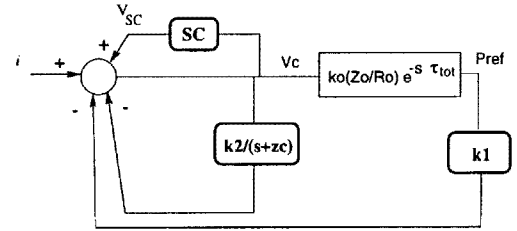$$B(s) = (s + z_c)(n_2(s) + k_1 k_0 Z_0(s)). \qquad (50)$$

Figure 4: A fixed low-order controller structure for $\tau_{tot} \neq 0$, $n^* \leq 2$

If $\tau_{tot} = 0$, then equation (46) gives that $n_1(s) = n_2(s)$. Therefore,

$$R_{cl}(s) = (s + z_c + k_2) R_0(s) + k_1 k_0(s + z_c) Z_0(s)$$
$$= A_0(s) \quad say. \qquad (51)$$

That is, the closed-loop polynomial coincides with that in equation (37), which was for the delay-free case. As shown in section 3.1, $A_0(s)$ is stable for certain choices of k_1 and k_2.

If $\tau_{tot} \neq 0$, we show that the controller structure given in figure 4 still guarantees stability. Since the polynomial $n_2(s)$ is of degree $n - 1$, its coefficients can be chosen such that

$$n_2(s) = -k_1 k_0 Z_0(s), \qquad (52)$$

which implies, from equation (50), that $B(s) = 0$ and therefore $R_{cl}(s) = A(s)$.

Furthermore, it is clear from equation (46) that the polynomials n_1 and n_2 of the SC are linked. More precisely, the choice of n_2 in (52) imposes restrictions on n_1: it means that the coefficients α_i, and hence n_1, are proportional to $k_0 k_1$. When $\tau_{tot} = 0$, $n_2 = n_1$, we will emphasise this scaling by writing:

$$n_2(s) = n_1(s) + \tau_{tot} k_0 k_1 n_3(s), \qquad (53)$$

where n_3 is a polynomial of degree $n - 1$, with finite coefficients. Therefore, using (52) and (53) in (48), the closed loop poles are the roots of

$$R_{cl}(s) = (s + z_c + k_2) R_0(s) + k_1 k_0(s + z_c) [Z_0(s) - \tau_{tot} n_3(s)] \qquad (54)$$

For 'small' τ_{tot}, ie for $\tau_{tot}\omega_a < O(1)$ where ω_a is the highest frequency among the zeros of Z_0, the zeros of $T(s) = Z_0(s) - \tau_{tot}n_3(s)$ are close to the zeros of $Z_0(s)$, and hence are stable. Therefore, for $|k_1|$ large, $n-1$ zeros of $R_{cl}(s)$ are stabilised. The 2 remaining zeros of $R_{cl}(s)$ are obtained at large s, $(k_1^{-1}(s + z_c + k_2)R_0(s)$ is not negligible compared to $(s + z_c)(Z_0(s) - \tau_{tot}n_3(s))$ when $s \geq O(k_1^{-1})$, and this is where we find the 2 remaining zeros of $R_{cl}(s)$). After division by s^{n-1} of the 3 highest coefficients of $R_{cl}(s)$, we obtain

$$s^2 + (k_2 - k_1 k_0 \tau_{tot} C)s + (k_1 k_0 - k_1 k_0 \tau_{tot} C z_c) \quad (55)$$

where C is the highest coefficient in $n_3(s)$. The 2 remaining roots of $R_{cl(s)}$ are stable if the polynomial (55) is stable, ie if

$$\begin{aligned} k_2 - k_1 k_0 \tau_{tot} C &> 0 \\ k_1 k_0 (1 - \tau_{tot} C z_c) &> 0. \end{aligned} \quad (56)$$

In the range of values of τ_{tot} considered (ie $\tau_{tot}\omega_a < O(1)$), one easily checks that $C \sim +1$ and that (56) is satisfied for some $k_1 > 0$ and $k_2 > 0$. Therefore, we proved that for 'small τ_{tot}', all the closed-loop poles, ie the roots of $R_{cl}(s)$, are stabilised for some $k_1 > 0$ and $k_2 > 0$. In other words, a plant of relative degree $n^* \leq 2$ with a time delay τ_{tot} not too large is stabilized by the controller structure given in figure 4, and the controller equation is given by:

$$V_c(t) = -k_1 P_{ref}(t) - \frac{k_2}{s + z_c}[V_c(t)] + \int_{-\tau_{tot}}^{0} \lambda(\sigma)V_c(t+\sigma)\,d\sigma. \quad (57)$$

In practice, the constraint on the size of τ_{tot} is not so strong: simulation results for a nonlinear model of an infinite order plant descibed in section 5, show that control is obtained with $k_1 > 0$ and $k_2 > 0$ for $\tau_{tot} \leq \frac{1}{\omega_u}$ where ω_u is the main unstable mode. Furthermore, for higher values of τ_{tot}, up to $\tau_{tot} \sim 3$ cycles of oscillations, we observe some periodic stability bands according to the values of $\omega_u \tau_{tot}$ (figure 5b): a 'stability band' corresponds to values of $\omega_u \tau_{tot}$ for which control is obtained after a finite time called settling time. Between two consecutive 'stability bands', there are a few values of $\omega_u \tau_{tot}$ for which control is not obtained (the settling time is then infinite). It was also observed that the sign of the first order compensator gain k_1 achieving control changes between two consecutive stability bands (see figure 5a). These observations on $sign(k_1)$ and on the stability bands pattern can be interpreted as follows: for frequencies smaller or equal to ω_u, the open-loop transfer function can be approximated by a second order system

$$k_0' \frac{1}{(s - \sigma_u)^2 + \omega_u^2} \quad (58)$$

where $k_0' = k_0(\sigma_u^2 + \omega_u^2)\frac{constant\ coefficient\ of\ Z_0}{constant\ coefficient\ of\ R_0}$ is a positive gain[§]. It is shown in appendix C that a plant of order 2, whose transfer function is given by (58), is stable for any delay τ_{tot} which satisfies

$$\begin{aligned} k_1 \sin(\omega_u \tau_{tot}) &< 0 \\ 1/\tan(\omega_u \tau_{tot}) - \frac{z_c}{\omega_u} &< 0. \end{aligned} \quad (59)$$

Hence, such a plant is characterized by a pattern of periodic stability bands according to the values of $\omega_u \tau_{tot}$, as shown in figure 5a. We see also from (59) that the sign of k_1 required for control satisfies

$$sign(k_1) = -sign(\sin(\omega_u \tau_{tot})), \quad (60)$$

which corresponds to observations from the simulation (see figure 5a). In a practical combustor, the time delay τ_{tot} would usually not exceed 3 cycles of oscillations, therefore our controller appears very adequate for control of combustion oscillations.

[§]the zeros of R_0 are complex conjugates, hence the constant coefficient of R_0 is positive. Z_0 is monic and stable, therefore its constant coefficient is also positive.
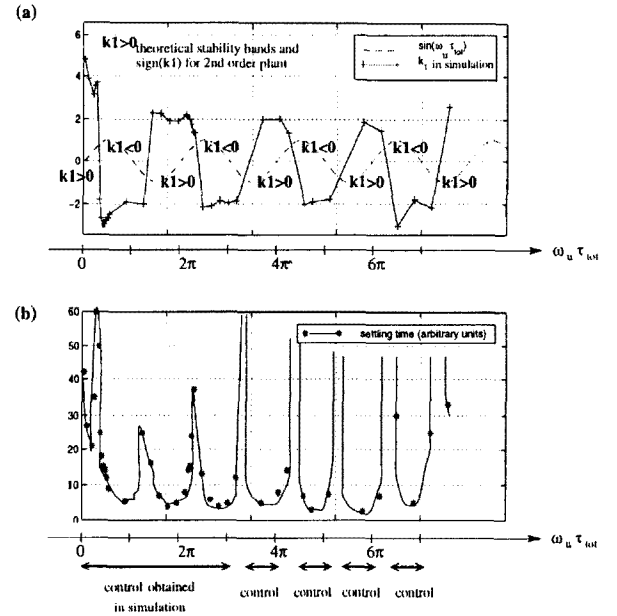

Figure 5: Comparison of simulation results for an infinite order plant (model described in section 5, $\omega_u = 370$ rad/s) with theoretical results for a second order plant (appendix C). (a) k_1 obtained in simulation and $sign(k_1)$ required for stability for a second order plant. (b) simulation: control obtained periodically up to $\omega_u \tau_{tot} \sim 3$ cycles of oscillations.

4. Adaptive regulator design

4.1 System without time delay $(\tau_{tot} = 0)$

It was shown in section 3.1 that a first order regulator $K_2(s) = k_c(s + z_c)/(s + p_c)$ will stabilize our combustion process which is minimum phase and of relative degree less or equal to 2. The adaptive version of this regulator, called Self-Tuning Regulator (STR), is given in figure 6.
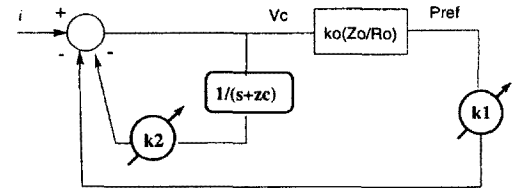

Figure 6: Low order adaptive controller for $\tau_{tot} = 0$, $n^* \leq 2$

With this controller structure, the closed-loop transfer function between some input noise i and P_{ref} is

$$\frac{P_{ref}(s)}{i(s)} = W_{cl}(s) = \frac{k_0(s + z_c)Z_0(s)}{R_{cl}(s)}, \quad (61)$$

and the closed-loop poles are the roots of

$$R_{cl}(s) = (s + z_c + k_2)R_0(s) + k_1 k_0(s + z_c)Z_0(s), \quad (62)$$

where $z_c > 0$ is fixed, and two controller parameters, $k_1(t)$ and $k_2(t)$, are tuned. It is clear from equations (62) and (37) that k_1 represents the gain k_c of the fixed regulator $K_2(s)$, while k_2 is used to tune p_c. In the following, vectors are denoted in bold characters and ^{T} denotes the transpose of a vector. We introduce:

- the unknown controller parameter vector $\mathbf{k}(t)^T = [-k_1(t), -k_2(t)]$, and the error parameter vector $\tilde{\mathbf{k}} = \mathbf{k} - \mathbf{k}^*$, where * denotes a value for which closed-loop stability is achieved.

- the data vector $\mathbf{d}(t)^T = [P_{ref}(t), V(t)]$, where $V(t) = \frac{1}{s+z_c}[V_c(t)]$ and z_c is a positive constant. In an experiment, $\mathbf{d}$ can be determined at each t from the measurement P_{ref} and known V_c.

We now need to find an updating rule for $\mathbf{k}$, so that stabilisation can be accomplished fo any parameters in $W_0(s)$.

Case (i) : $n^*(W_0) = 1$. This corresponds to a case for which Narendra & Annaswamy [21] have developed a STR. However, we will repeat the main points of their argument because they provide the background to our novel STR for the case with time delay in section 4.2. When $n^*(W_0) = 1$, the closed-loop transfer function W_{cl} given in (61) has then a relative degree equal to 1 and is 'Strictly Positive Real' (SPR), which is the essential property required to develop a global stability analysis based on Lyapunov's direct method [21]. Such a method aims at finding adaptive laws for $\mathbf{k}$ which are guaranteed to stabilize the self-excited combustion process. Essentially, the strictly positive realness of W_{cl} means that it is possible to find a quadratic positive function V_l, that decays in time when $\mathbf{k}$ is updated correctly. Such a function V_l is referred to as a 'Lyapunov function', and can be viewed as an energy function: if this function decreases, it implies that the system is stabilised. To summarize Narendra & Annaswamy's results [21], when W_0 has a relative degree equal to 1, the STR which guarantees the stability of the system is described by:

$$
\begin{aligned}
V_c(t) &= \mathbf{k}^T(t).\mathbf{d}(t) \\
\dot{\mathbf{k}}(t) &= -sign(k_0)P_{ref}(t)\mathbf{d}(t),
\end{aligned}
\tag{63}
$$

where $sign(k_0) = +1$ from Lemma 3. For reference, equation (63) comes from the application of lemma 5.1 in Narendra & Annaswamy [21], noting that

$$
P_{ref}(t) = W_{cl}(s)[\tilde{\mathbf{k}}^T(t).\mathbf{d}(t)].
\tag{64}
$$

Case (ii) : $n^*(W_0) = 2$. In this case W_{cl} is not SPR, but the approach of Annaswamy et al [2] shows that modifying the control signal V_c as indicated in figure 7 effectively makes the closed-loop transfer function W_{cl} have relative degree 1. Following their approach, we write

$$
V_c(t) = (s+a)[\mathbf{k}^T(t).\mathbf{d_a}(t)]
\tag{65}
$$

where $\mathbf{d_a}(t) = \frac{1}{s+a}[\mathbf{d}(t)]$. After some simple algebra, V_c can be written as

$$
V_c(t) = \mathbf{k}^T(t).\mathbf{d}(t) + \dot{\mathbf{k}}^T(t).\mathbf{d_a}(t).
\tag{66}
$$

Now, we have

$$
\begin{aligned}
P_{ref}(t) &= W_{cl}(s)(s+a)[\tilde{\mathbf{k}}^T(t).\mathbf{d_a}(t)] \\
&= W_m(s)[\tilde{\mathbf{k}}^T(t).\mathbf{d_a}(t)],
\end{aligned}
\tag{67}
$$

where $W_m(s) = (s+a)W_{cl}(s)$ is the new closed-loop transfer function of our system, which has relative degree 2 and is SPR. Noting that equation (67) looks similar to equation (64), lemma 5.1 [21] can be applied: the STR which will guarantee the stability of the system of relative degree 2 is given by:

$$
\begin{aligned}
V_c(t) &= \mathbf{k}^T(t).\mathbf{d}(t) + \dot{\mathbf{k}}(t)^T.\mathbf{d_a}(t) \\
\dot{\mathbf{k}}(t) &= -sign(k_0)P_{ref}(t)\mathbf{d_a}(t),
\end{aligned}
\tag{68}
$$

where $sign(k_0) = +1$ from Lemma 3.

An important remark is that the STR described for the case $n^*(W_0) = 2$ will also work if $n^*(W_0) = 1$, which means that even if the actuator dynamics are not very well known in practice, the STR design given in equation (68) will always give satisfactory results.
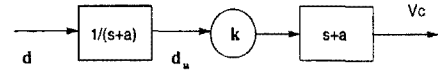

Figure 7: Modification of the control input V_c

4.2 Combustion system with known time delay $(\tau_{tot} \neq 0)$

The controller structure given in figure 4 includes fixed controller parameters k_1, k_2, α_i and β_i which need to be chosen based on the system parameters. Under uncertainties and variations in the operating conditions, it is more appropriate to adapt those control parameters. Hence, we choose an adaptive controller structure as shown in figure 8.
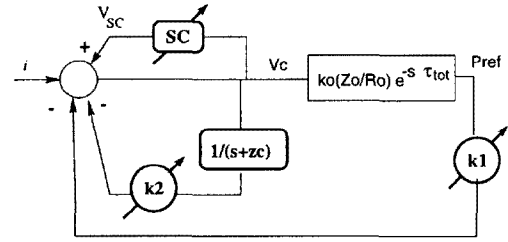

Figure 8: A low-order adaptive controller for $\tau_{tot} \neq 0$, $n^* \leq 2$

In the control law given in equation (57), the finite-time integral due to Smith Controller and given in equation (42) is approximated as follows:

$$
V_{SC}(t) = \sum_{i=1}^{N} \lambda_i(t)V_c(t - idt).
\tag{69}
$$

Similar to the delay-free case, we define the controller parameters and data vectors $\mathbf{k}$ and $\mathbf{d}$ respectively:

- $\mathbf{k}(t)^T = [-k_1(t), -k_2(t), \lambda_N(t), ..., \lambda_1(t)]$, and its error vector $\tilde{\mathbf{k}} = \mathbf{k} - \mathbf{k}^*$.
- $\mathbf{d}(t)^T = [P_{ref}(t), V(t), V_c(t - Ndt), ..., V_c(t - dt)]$, where $V(t) = \frac{1}{s+z_c}[V_c(t)]$.

Therefore, as the time delay τ_{tot} is increased, N must be increased and more controller parameters are required. We are looking for an updating rule for $\mathbf{k}$.

General case : $n^*(W_0) \leq 2$. As in section 4.1, the closed loop transfer function W_{cl_0} given in (47) is made to effectively have relative degree 1 by using a modified control signal V_c (see figure 7). Then we obtain:

$$
P_{ref}(s) = W_{cl_0}(s)(s+a)e^{-s\tau_{tot}}[\tilde{\mathbf{k}}^T(t).\mathbf{d_a}(t)],
\tag{70}
$$

where $\mathbf{d_a}(t) = \frac{1}{s+a}[\mathbf{d}(t)]$. Due to the presence of the time delay $e^{-s\tau_{tot}}$, the Lyapunov function V_l used in the delay-free case will not decay in time. So we need to add an extra positive term in V_l, in the form of a double integral $\int_{-\tau_{tot}}^{0} \int_{t+\nu}^{t} \|\dot{\tilde{\mathbf{k}}}(\xi)\|^2 d\xi d\nu$, to account for the time delay τ_{tot}. Then we have $\dot{V}_l \leq 0$, and hence a system whose energy is decaying in time (see details of proof in Appendix D). Therefore, with the Lyapunov function given in equation (98), the stability of the system is guaranteed when one uses the following STR:

$$
\begin{aligned}
V_c(t) &= \mathbf{k}^T(t).\mathbf{d}(t) + \dot{\mathbf{k}}(t)^T.\mathbf{d_a}(t) \\
\dot{\mathbf{k}}(t) &= -sign(k_0)P_{ref}(t)\mathbf{d_a}(t - \tau_{tot}),
\end{aligned}
\tag{71}
$$

where $sign(k_0) = +1$.

Particular case : $n^*(W_0) = 1$. Then the manipulation on V_c shown in figure 7 is not required, and therefore the following simpler algorithm can be implemented:

$$V_c(t) = \mathbf{k}^T(t).\mathbf{d}(t)$$
$$\dot{\mathbf{k}}(t) = -sign(k_0)P_{ref}(t)\mathbf{d}(t - \tau_{tot}), \qquad (72)$$

where $sign(k_0) = +1$.

5. Application to a premixed ducted flame (simulation)

5.1 Nonlinear flame model used in the simulation

A model for nonlinear oscillations of a ducted flame developed by Dowling [10] will be used to verify the controller performance. The theory involves extension of the flame model of Fleifil et al[13] to include a flame holder at the centre of the duct and nonlinear effects. Due to page limitations, the reader is asked to refer to [10] for details.

5.2 Adaptive regulator design

The flame model described in [10] fits in the class of combustion systems given in section 2, since:

- the upstream reflection coefficient has a modulus strictly smaller than 1 (choked end: $R_u = (1 - \bar{M}_1)/(1 + \bar{M}_1)$) , in agreement with equation 3. Notice that the downstream reflection coefficient has modulus just equal to 1 (ideal open end: $R_d = -1$). However, with care the condition $|R_d(s)| < 1$ in equation 3 can be relaxed to $|R_d(s)| \leq 1$ provided an upstream pressure measurement is made. This is because in the transfer function $G(s)$ given in (7), $|X_{12}| > |Y_{12}|$ and $|X_{22}| > |Y_{22}|$.

- after linearisation for small perturbations, the flame transfer function is given by (see [10]):

$$H(s) = \frac{Q_n(s)}{u_G(s)} = \frac{2\eta\Delta H e^{-s\tau_2}}{s\tau_f \bar{c}_1^2(b+a)} \left[a - be^{-s\tau_f} + \frac{b-a}{s\tau_f}(1 - e^{-s\tau_f})\right] \qquad (73)$$

Therefore, $H \to 0$ as $s \to \infty$, and $H(s)$ has no poles: hence assumptions (I) and (II) are satisfied.

Hence, section 2 proves that, once the system is approximated as finite dimensional, the relative degree of the open-loop transfer function W_0 is equal to the relative degree of the actuator transfer function. As in Evesque et al [11], the actuator chosen is a fuel injection system modelled as follows:

$$\frac{Q_c(s)}{V_c(s)} = \frac{e^{-s\tau_a}}{s^2/\omega_c^2 + 2cs/\omega_c + 1} \qquad (74)$$

where ω_c and c are respectively the resonance frequency and damping of the fuel injector. From equation (74), we deduce that the relative degree of W_0 is 2. Section 2 shows also that the 'high frequency gain' k_0 is positive and that the zeros of W_0 are stable.

Two cases are studied in the simulation:

- a system without time delay ($\tau_{tot} = 0$). This is achieved by making the pressure measurement at the flame (ie $x_{ref} = 0$) and by setting the time delay τ_a to zero in equation (74). Then the STR is implemented as indicated in equation (68), with $sign(k_0) = +1$.

- a system with time delay ($\tau_{tot} \neq 0$). The pressure measurement is chosen for instance at $x_{ref} = -x_u/2$ and the delay τ_a can be varied. Then the adequate STR to control the self-excited oscillations is given in equation (71), with $sign(k_0) = +1$.

For both cases, a convergence coefficient μ is added in the adaptive law for each controller parameter. The controller parameter vector $\mathbf{k}$ is initialized to zero. Simulations results are given in the next section.

5.3 Simulation results

System without time delay ($\tau_{tot} = 0$). Figure 9 shows the time evolution of the pressure measurement P_{ref} and the corresponding control signal V_c for varying operating conditions. The control is switched on at $t = 0.15$ s, when the limit cycles are already established (operating conditions: $\phi = 0.7$, $\bar{M}_1 = 0.08$). The oscillations tend to zero within 1 s; note that the settling time depends on the convergence coefficient μ used. Then from $t = 1.95$ s to $t = 2.1$ s, $\bar{M}_1$ is increased to 0.095: in the open-loop system such a change shifts the frequency of the unstable mode from 58 to 63 Hz. Nevertheless, the STR is able to maintain control. Changes in the fuel air ratio ϕ have also been successfully tested. It has been observed that the STR works fine even if x_{ref} is chosen anywhere upstream the flame, which is interesting for practical applications where a pressure measurement directly at the flame may be difficult to perform.
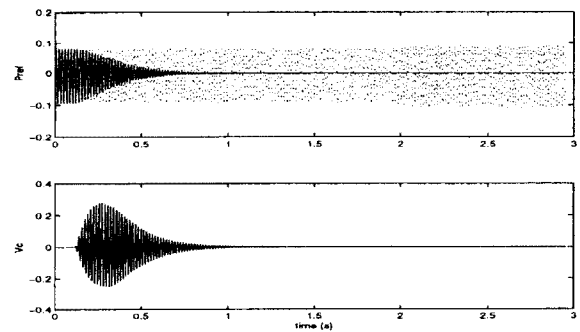

Figure 9: STR for $\tau_{tot} = 0$, $\bar{M}_1$ is varied linearly from 0.08 at $t = 1.95$ s to 0.095 at $t = 2.1$ s. ...: controller OFF, —: controller ON after $t = 0.15$ s.

System with time delay ($\tau_{tot} \neq 0$). This is the most interesting case for practical applications. As already illustrated in section 3 (see figure 5), control is obtained for values of τ_{tot} much larger than those predicted by the theory: control is achieved periodically up to $\tau_{tot} \sim 3$ cycles of oscillations (ie up to $\omega_u\tau_{tot} \sim 6\pi$ where ω_u is the unstable mode). The settling time varies periodically: control is easier in the middle of a stability band, and becomes more difficult on the boundaries of a stability bands. As in the delay free case ($\tau_{tot} = 0$), the actual value of the settling time depends on the convergence coefficient μ chosen. A typical time evolution of the pressure oscillations while control is applied is shown in figure 10. There, in order to test the adaptability of our STR under varying operating conditions, the mean upstream Mach number $\bar{M}_1$ is increased from 0.08 to 0.095 between $t = 1.95$ s and $t = 2.1$ s: the STR successfully maintains P_{ref} at zero.

6. Conclusions

A general combustion system, susceptible to combustion instabilities, and satisfying the following assumptions, was considered:

1. the pressure reflection coefficients at the boundaries of the combustor have a modulus strictly smaller than 1 in $Real(s) \geq 0$.

2. the flame response has a limited bandwidth: at high frequencies, the flame does not follow incoming velocity fluctuations.

3. the flame is stable in itself, it becomes unstable only due to the interaction with the acoustic waves in the combustor.
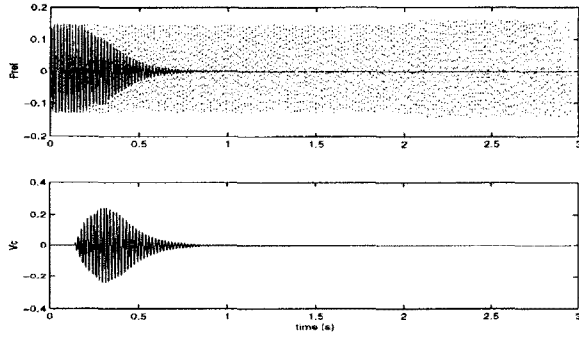
Figure 10: STR for $\tau_{tot} = 23$ ms, $x_{ref} = -x_u/2$, $\overline{M}_1$ is varied linearly from 0.08 at $t = 1.95$ s to 0.095 at $t = 2.1$ s. ... : controller OFF, — : controller ON after $t = 0.15$ s.

4. the actuator used for control is a fuel injector which produces a heat release rate Q_c related to the voltage V_c driving the actuator simply by a time delay and a first or second order differential equation.

We demonstrated that such a combustion system is essentially represented by an open-loop transfer function

$$W(s) = \frac{P_{ref}(s)}{V_c(s)} = k_0 \frac{Z_0(s)}{R_0(s)} e^{-s\tau_{tot}}$$

where P_{ref} is a pressure measurement in the combustor and V_c is the voltage driving the fuel injector used as control actuation. Some general properties have been derived:
(i) the zeros of $Z_0(s)$ are all stable (ie are in $Real(s) < 0$)
(ii) Once Z_0/R_0 has been made rational using a Padé expansion, the relative degree of $Z_0(s)/R_0(s)$ is equal to the relative degree of the actuator transfer function, ie 2 for a fuel injector.
(iii) k_0 is a positive gain.
These properties have been exploited to design an adaptive controller guaranteed to stabilise the self-excited combustion system. In particular, for the case of a combustion system with time delay ($\tau_{tot} \neq 0$), which is the most realistic case, the design is completely novel: it involves a first order compensator combined with a Smith Controller. The adaptive laws for the controller parameters are derived based on a Lyapunov stability analysis. The adaptive controller has been tested successfully on a simulation of a premixed ducted flame. An experimental verification is planned over the next months.

ACKNOWLEDGMENTS

APPENDIX

Appendix A. Consider linear disturbances with time dependence e^{st} in the pipework system upstream the combustion zone, as shown in figure 11. The Mach number considered is so low that we assume there is no mean flow in the pipework system. The pressure reflection coefficient at an axial position x_i is $R_{u_i}(s)$. The cross-sectional area of the duct i between $x = x_i$ and $x = x_{i+1}$ is A_i. The mean speed of sound is $\bar{c}$ and the mean density is $\bar{\rho}$. At x_0, we assume that the pressure reflection coefficient $R_{u_0}(s)$ satisfies

$$
\begin{aligned}
|R_{u_0}(s)| &< 1 \quad in \quad Real(s) \geq 0 \\
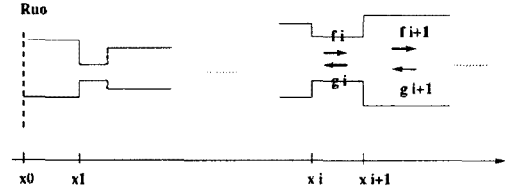n^*(R_{u_0}(s)) &= 0.
\end{aligned}
\tag{75}
$$

Figure 11: upstream pipework system

These assumptions are true for a choked end at $x = x_0$ for instance. In the following, we show by induction that for all i, $|R_{u_i}(s)| < 1$ in $Real(s) \geq 0$, and $n^*(R_{u_i}(s)) = 0$.

At $x = x_i$, the reflected wave f_i is related to the incoming wave g_i:

$$f_i(t) = e^{-2s\frac{x_{i+1}-x_i}{\bar{c}}} R_{u_i}(s)[g_i(t)]. \tag{76}$$

Writing the continuity of pressure and mass flux across $x = x_{i+1}$, and using the boundary condition (76) leads to the following relationship between the reflected wave f_{i+1} and the incoming wave g_{i+1} in the duct $i + 1$:

$$f_{i+1}(t) = e^{-2s\frac{x_{i+2}-x_{i+1}}{\bar{c}}} R_{u_{i+1}}(s)[g_{i+1}(t)], \tag{77}$$

where

$$R_{u_{i+1}}(s) = \frac{K_i + R_{u_i}(s)e^{-s\tau_i}}{1 + K_i R_{u_i}(s)e^{-s\tau_i}} \tag{78}$$

$$K_i = \frac{A_{i+1} - A_i}{A_{i+1} + A_i} \tag{79}$$

$$\tau_i = \frac{-2(x_{i+1} - x_i)}{\bar{c}}. \tag{80}$$

By inspection $|K_i| < 1$. Furthermore, from (78), one deduces that $n^*(R_{u_i}(s)) = 0$ implies that $n^*(R_{u_{i+1}}(s)) = 0$ after a Padé expansion $[M/M]$ for $e^{-s\tau_i}$ is made. Let us write R_{u_i} in the form $R_{u_i}(s) = |R_{u_i}(s)|e^{-s\alpha_i}$ in equation (78). Then one easily obtains

$$|R_{u_{i+1}}(s)|^2 = \frac{K_i^2 + |R_{u_i}|^2 e^{-2\delta_i} + 2K_i|R_{u_i}(s)|e^{-\delta_i}\cos(\theta_i)}{1 + K_i^2|R_{u_i}|^2 e^{-2\delta_i} + 2K_i|R_{u_i}(s)|e^{-\delta_i}\cos(\theta_i)} \tag{81}$$

where $\theta_i = Imag(s)\tau_i + \alpha_i$ and $\delta_i = Real(s)\tau_i$.
The difference P between the numerator and the denominator of $|R_{u_{i+1}}(s)|^2$ is equal to

$$P = (1 - K_i^2)(|R_{u_i}|^2 e^{-2Real(s)\tau_i} - 1) \tag{82}$$

Therefore, in $Real(s) \geq 0$, $|R_{u_i}(s)| < 1$ implies that $P < 0$ and hence $|R_{u_{i+1}}| < 0$.

Now we assume that at $x = x_0$, the high frequency gain h_0 of $R_{u_0}(s)$ satisfies

$$|h_0| < 1. \tag{83}$$

(this is true for a choked end). We show by induction that for all i, the high frequency gain h_i of $R_{u_i}(s)$ satisfies $|h_i| < 1$.
From (78), after a Padé expansion $[M/M]$ for $e^{-s\tau_i}$ is made, one deduces that

$$h_{i+1} = \frac{K_i + h_i(-1)^M}{1 + K_i h_i(-1)^M}. \tag{84}$$

and hence

$$|h_{i+1}^2| = \frac{K_i^2 + h_i^2 - 2(-1)^M K_i h_i}{1 + 2K_i h_i(-1)^M + K_i^2 h_i^2}. \tag{85}$$

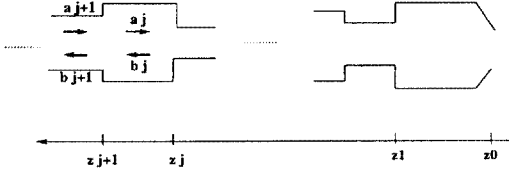The difference Q between the numerator and the denominator of h_{i+1} is

Figure 12: downstream pipework system

Figure 13: $sign(k_1)$ and values of $\omega_u \tau_{tot}$ for which a plant of order 2 is guaranteed to be stabilised by the fixed controller described in figure 4

$$Q = (1 - K_i^2)(h_i^2 - 1). \tag{86}$$

Hence, $|h_i| < 1$ implies that $Q < 0$ and therefore $|h_{i+1}| < 1$.

Similarly, for a pipework system downstream the flame, ended by a nozzle (see figure 12), we assume that at $z = z_0$, the pressure reflection coefficient R_{d_0} satisfies the assumptions (75) and (83), which is true if the nozzle is compact [20]. By induction, it can be shown that at any position $z = z_j$, the downstream pressure coefficient R_{d_j} and its high frequency gain h_j satisfy

$$
\begin{aligned}
n^*(R_{d_j}) &= 0 \\
|R_{d_j}(s)| &< 1 \quad in \quad Real(s) \geq 0 \\
|h_j| &< 1.
\end{aligned} \tag{87}
$$

Appendix B. The full form of the coefficients in equation (7) is:

$$
\mathbf{X} = \begin{pmatrix} -1 + \bar{M}_1 \left(2 - \frac{\bar{u}_2}{\bar{u}_1}\right) - \bar{M}_1^2 \left(1 - \frac{\bar{u}_2}{\bar{u}_1}\right) & 1 + \bar{M}_1 \frac{\bar{\rho}_1 \bar{c}_1}{\bar{\rho}_2 \bar{c}_2} \\ \frac{1 - \gamma \bar{M}_1}{\gamma - 1} + \bar{M}_1^2 - \bar{M}_1^2 (1 - \bar{M}_1) \frac{1}{2} \left(\frac{\bar{u}_2^2}{\bar{u}_1^2} - 1\right) & \frac{\bar{c}_2}{\bar{c}_1} \frac{1 + \gamma \bar{M}_2}{\gamma - 1} + \bar{M}_1 \bar{M}_2 \frac{\bar{\rho}_1}{\bar{\rho}_2} \end{pmatrix} \tag{88}
$$

$$
\mathbf{Y} = \begin{pmatrix} 1 + \bar{M}_1 \left(2 - \frac{\bar{u}_2}{\bar{u}_1}\right) + \bar{M}_1^2 \left(1 - \frac{\bar{u}_2}{\bar{u}_1}\right) & \bar{M}_1 \frac{\bar{\rho}_1 \bar{c}_1}{\bar{\rho}_2 \bar{c}_2} - 1 \\ \frac{1 + \gamma \bar{M}_1}{\gamma - 1} + \bar{M}_1^2 - \bar{M}_1^2 (1 + \bar{M}_1) \frac{1}{2} \left(\frac{\bar{u}_2^2}{\bar{u}_1^2} - 1\right) & \frac{\bar{c}_2}{\bar{c}_1} \frac{1 - \gamma \bar{M}_2}{\gamma - 1} + \bar{M}_1 \bar{M}_2 \frac{\bar{\rho}_1}{\bar{\rho}_2} \end{pmatrix} \tag{89}
$$

Appendix C. Consider an unstable plant of order 2, defined by $Z_0(s) = 1$ and $R_0(s) = (s - \sigma_u)^2 + \omega_u^2$ ($\sigma_u < 0$ for an unstable mode), and whose total time delay is τ_{tot}. Using the controller defined in figure 4, the denominator of the closed-loop transfer function is easily calculated analytically and is found to be:

$$R_{cl}(s) = s^3 + as^2 + bs + c \tag{90}$$

where

$$
\begin{aligned}
a &= -2\sigma_u + z_c + k_2 - k_0 k_1 \frac{\sin(\omega_u \tau_{tot})}{\omega_u} \\
b &= \sigma_u^2 + \omega_u^2 - 2\sigma_u(z_c + k_2) + k_0 k_1 e^{-\sigma_u \tau_{tot}} \left[\frac{\sigma_u - z_c}{\omega_u} \sin(\omega_u \tau_{tot}) + \cos(\omega_u \tau_{tot})\right] \\
c &= (\sigma_u^2 + \omega_u^2)(z_c + k_2) + k_0 k_1 e^{-\sigma_u \tau_{tot}} z_c \left[\frac{\sigma_1}{\omega_u} \sin(\omega_u \tau_{tot}) + \cos(\omega_u \tau_{tot})\right] \quad (91)
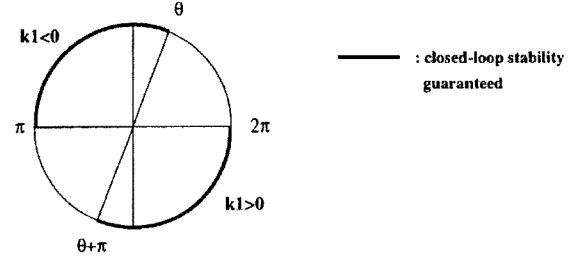\end{aligned}
$$

Assuming that $|\sigma_u| \ll \omega_u$ (realistic assumption: the growth rate is much smaller than the frequency of the unstable mode), the Routh criteria applied to $R_{cl}(s)$ shows that $R_{cl}(s)$ is stable for some $k_2 > 0$ if

$$
\begin{aligned}
k_1 \sin(\omega_u \tau_{tot}) &< 0 \\
1/\tan(\omega_u \tau_{tot}) - \frac{z_c}{\omega_u} &< 0.
\end{aligned} \tag{92}
$$

Consider the angle θ defined by $\frac{1}{\tan(\theta)} = \frac{z_c}{\omega_u}$ and $\sin(\theta) > 0$. Then, as illustrated in figure 13:

- for $\theta < \omega_u \tau_{tot} < \pi/2$ and $k_1 < 0$, $R_{cl}(s)$ is stable.
- for $\theta + \pi < \omega_u \tau_{tot} < 2\pi$ and $k_1 > 0$, $R_{cl}(s)$ is stable.

Hence the periodic stability bands shown in figure 5a. Also note the result that k_1 required for control satisfies $sign(k_1) = -sign(\sin(\omega_u \tau_{tot}))$.

Appendix D. We start from equation (70):

$$P_{ref}(t) = W_m(s) e^{-s\tau_{tot}} [\tilde{\mathbf{k}}^T(t).\mathbf{d_a}(t)], \tag{93}$$

where $W_m(s) = W_{cl_0}(s)(s + a)$ is SPR and $\mathbf{d_a}(t) = \frac{1}{s+a}[\mathbf{d}(t)]$.

The adaptive law is chosen as

$$\dot{\mathbf{k}}(t) = -P_{ref}(t)\mathbf{d_a}(t - \tau_{tot}) \tag{94}$$

(a positive sign for k_0 is assumed).

Equation (93) can be expressed in a state-variable representation as

$$
\begin{aligned}
\dot{\mathbf{x}} &= A\mathbf{x}(t) + (s + a) \left[\mathbf{b}(\tilde{\mathbf{k}}^T(t - \tau_{tot}).\mathbf{d_a}(t - \tau_{tot}))\right] \\
P_{ref}(t) &= \mathbf{h}^T.\mathbf{x}(t).
\end{aligned} \tag{95}
$$

$\mathbf{x}$ is the 'state vector' of the system and A is a matrix. $(A, \mathbf{b}, \mathbf{h})$ is the 'state representation' of W_0.

We note that equation (95) can be rewritten as

$$
\begin{aligned}
\dot{\mathbf{x}}(t) = A\mathbf{x} &+ (s + a) \left[\mathbf{b} \left(\tilde{\mathbf{k}}^T(t).\mathbf{d_a}(t - \tau_{tot})\right)\right] \\
&- (s + a) \left[\mathbf{b}\mathbf{d_a}^T(t - \tau_{tot}) \left(\int_{-\tau_{tot}}^{0} \dot{\tilde{\mathbf{k}}}(t + \nu) d\nu\right)\right].
\end{aligned} \tag{96}
$$

Using equation (94), this leads to

$$
\begin{aligned}
\dot{\mathbf{x}}(t) = A\mathbf{x} &+ (s + a) \left[\mathbf{b} \left(\tilde{\mathbf{k}}^T(t).\mathbf{d_a}(t - \tau_{tot})\right)\right] \\
&+ (s + a) \left[\mathbf{b}\mathbf{d_a}^T(t - \tau_{tot}) \left(\int_{-\tau_{tot}}^{0} P_{ref}(t + \nu)\mathbf{d_a}(t + \nu - \tau_{tot}) d\nu\right)\right].
\end{aligned} \tag{97}
$$

As in Burton [7] and Niculescu [23] [22], the Lyapunov function candidate is chosen as

$$V_l = \mathbf{x}^T(t) P\mathbf{x}(t) + \tilde{\mathbf{k}}^T(t)\tilde{\mathbf{k}}(t) + \int_{-\tau_{tot}}^{0} \int_{t+\nu}^{t} \|\dot{\tilde{\mathbf{k}}}(\xi)\|^2 d\xi d\nu. \tag{98}$$

Using equations (94) and (97), equation (98) leads to the time-derivative

$$
\begin{aligned}
\dot{V}_l = \mathbf{x}^T(A^T P + P^T A)\mathbf{x} &+ 2\mathbf{x}^T(t) P(s + a) \left[\mathbf{b} \left(\tilde{\mathbf{k}}^T(t).\mathbf{d_a}(t - \tau_{tot})\right)\right] \\
&+ 2\mathbf{x}^T(t) P(s + a) \left[\mathbf{b}\mathbf{d_a}(t - \tau_{tot}) \left(\int_{-\tau_{tot}}^{0} P_{ref}(t + \nu)\mathbf{d_a}(t + \nu - \tau_{tot}) d\nu\right)\right] \\
&- 2P_{ref}(t)\tilde{\mathbf{k}}^T(t).\mathbf{d_a}(t - \tau_{tot}) + \frac{d}{dt}\left[\int_{-\tau_{tot}}^{0} \int_{t+\nu}^{t} (P_{ref}(\xi))^2 \|\mathbf{d_a}(\xi - \tau_{tot})\|^2 d\xi d\nu\right] \quad (99)
\end{aligned}
$$

Since $W_m(s)$ is SPR, lemma 2.4 [21] can be used: given a matrix Q symmetric strictly positive, there exists a matrix P symmetric strictly positive, such that

$$A^T P + P^T A = -Q, \qquad P(s+a)\mathbf{b} = \mathbf{h}, \qquad (100)$$

which leads to

$$\dot{V}_l = -\mathbf{x}^T Q \mathbf{x} + 2 P_{ref}(t) \mathbf{d_a}(t-\tau_{tot}) \left(\int\limits_{-\tau_{tot}}^{0} P_{ref}(t+\nu) \mathbf{d_a}(t+\nu-\tau_{tot}) d\nu \right)$$

$$+ \int\limits_{-\tau_{tot}}^{0} \left[\|P_{ref}(t)\mathbf{d_a}(t-\tau_{tot})\|^2 - \|P_{ref}(t+\nu)\mathbf{d_a}(t+\nu-\tau_{tot})\|^2 \right] d\nu. \quad (101)$$

Denoting

$$\mathbf{y} = P_{ref}(t)\mathbf{d_a}(t-\tau_{tot}), \qquad \mathbf{z} = P_{ref}(t+\nu)\mathbf{d_a}(t+\nu-\tau_{tot}), \quad (102)$$

equation (101) can be rewritten as

$$
\begin{aligned}
\dot{V}_l &= -\mathbf{x}^T Q \mathbf{x} + \int\limits_{-\tau_{tot}}^{0} \left(2\mathbf{y}^T \mathbf{z} + \mathbf{y}^T \mathbf{y} - \mathbf{z}^T \mathbf{z} \right) d\nu \\
&= -\mathbf{x}^T Q \mathbf{x} - \int\limits_{-\tau_{tot}}^{0} \left(\|\mathbf{z} - \mathbf{y}\|^2 - 2\mathbf{y}^T \mathbf{y} \right) d\nu \\
&\leq -\mathbf{x}^T Q \mathbf{x} + 2\tau_{tot} \|P_{ref}(t)\mathbf{d_a}(t-\tau_{tot})\|^2 \\
&\leq -P_{ref}^2(t)\left(k - 2\tau_{tot} \|\mathbf{d_a}(t-\tau_{tot})\| \right) \\
&\leq 0 \qquad for \quad \|\mathbf{d_a}\| \leq k/2\tau_{tot}. \qquad (103)
\end{aligned}
$$

Therefore, the stability of the delayed plant under control is guaranteed for all τ_{tot}. A domain of attraction results, given by $\|P_{ref}\mathbf{d_a}\| \leq k/2\tau_{tot}$; this domain reaches $\mathbb{R}^n$ as $\tau_{tot} \to 0$.

[1] AM Annaswamy, M Fleifil, JW Rumsey, JP Hathout, and AF Ghoniem. An input-output model of thermoacoustic instability and active control design. Technical report, MIT, 1997.

[2] A.M. Annaswamy, O.M. El Rifai, M. Fleifil, and A.F. Ghoniem J.P. Hathout. A model-based self-tuning controller for thermoacoustic instability. *Combust. Sci. and Tech.*, 135:213–240, 1998.

[3] G.A. Baker, Jr and P. Graves-Morris. *Pade approximants, 2nd edition*. Cambridge University Press, 1996.

[4] A Banaszuk, CA Jacobson, AI Khibnik, and PG Mehta. Linear and nonlinear analysis of controlled combustion processes. In *Proceedings of the 1999 IEEE Internation Conference on Control Applications*, Hawai'i, USA, August 1999.

[5] G Billoud, MA Galland, C Huynh Huu, and S Candel. Adaptive control of combustion instabilities. *Combust Sci Tech*, 81:257–283, 1992.

[6] R Blonbou, S Zaleski, A Laverdant, and P Kuentzmann. Active adaptive combustion control using neural networks. To be published in *Combust Sci Tech* in 2000.

[7] T.A. Burton. *Stability and periodic solutions of ordinary and functional differential equations*. Academic Press, Orlando, 1985.

[8] R Dorf and R Bishop. *Modern control systems (7th edition)*. Addison Wesley, 1995.

[9] AP Dowling. Nonlinear self-excited oscillations of a ducted flame. *J Fluid Mech*, 346:271–290, 1997.

[10] AP Dowling. A kinematic model of a ducted flame. *J. Fluid Mech.*, 394:51–72, 1999.

[11] S. Evesque, Y.C. Chu, A.P. Dowling, and K. Glover. Feedback control of a premixed ducted flame. In *Proceedings of the ISABE XIV International Symposium*, Florence, Italy, September 1999. Paper IS-7187.

[12] S Evesque and AP Dowling. Lms algorithm for adaptive control of combustion oscillations. Submitted to *Combust Sci Tech* in 1999.

[13] M Fleifil. Response of a laminar premixed flame to flow oscillations : a kinematic model and thermoacoustic instabilities results. *Combust Flame*, 106:487–510, 1996.

[14] S Hubbard and AP Dowling. Acoustic instabilities in premix burners. 4th AIAA/CEAS Aeroacoustics Conference, Toulouse, June 1998, 1998.

[15] K. Ichikawa. Frequency-domain pole assignment and exact model-matching for delay systems. *Int J Control*, 41(4):1015–1024, 1985.

[16] K. Ichikawa. Adaptive control of delay system. *Int. J. Control*, 43(6):1653–1659, 1986.

[17] A Kemal and CT Bowman. Real time adaptive feedback control of combustion instability. In *Twenty-Sixth Symposium (International) on Combustion*, pages 2803–2809, 1996.

[18] PJ Langhorne, AP Dowling, and N Hooper. Practical active control system for combustion oscillations. *J Prop Power*, 6:324–330, 1990.

[19] AZ Manitius and AW Olbrot. Finite spectrum assignment problem for systems with delays. *IEEE transactions on automatic control*, AC-24:541–553, 1979.

[20] F.E. Marble and S.M. Candel. Acoustic disturbance from gas non-uniformities convected through a nozzle. *Journal of Sound and Vibration*, 55(2):225–243, 1977.

[21] K.S. Narendra and A.M. Annaswamy. *Stable Adaptive Systems*. Prentice-Hall International, 1989.

[22] S.I. Niculescu. *Qualitative aspects on the stability and stabilization*. (in French), Diderot, Paris, Nouveaux Essais, 1997.

[23] S.I. Niculescu, E.I. Verriest, L.Dugard, and J.M.Dion. *Stability and control of time-delay systems*, chapter "Stability and robust stability of time-delay systems: A guided tour". (Ed: Dugard and Verriest), LNCIS, Springer-Verlag, London, 1997.

[24] R Ortega and R Lozano. Globally stable adaptive controller for system with delay. *Int J Contr*, 47:17–23, 1988.

[25] KT Padmanabhan, CT Bowman, and J David Powell. On-line adaptive optimal combustor control. *IEEE transactions on control systems technology*, 4(3), May 1996.

[26] CO Paschereit, E Gutmark, and W Weisenstein. Control of thermoacoustic instabilities in a premixed combustor by fuel modulation. In *37th AIAA Aerospace Science Meeting and Exhibit*, Reno, Nevada, January 1999.

[27] T Poinsot, C Le Chatelier, SM Candel, and E Esposito. Experimental determination of the reflection coefficient of a premixed flame in a duct. *Journal of Sound and Vibration*, 107(2):265–278, 1986.

[28] W.H. Press, S.A. Teukolsky, W.T. Vetterling, and B.P. Flannery. *Numerical Recipes, 2nd ed.* Cambridge University Press, New York, 1992.

[29] GA Richard and MC Janus. Characterization of oscillations during premix gas turbine combustion. *ASME J. Eng. for Gas Turbines and Power*, 120:294–302, 1998.

[30] OJM Smith. A controller to overcome dead time. *ISA*, 6(2):28–33, 1959.

PAPER -22, S. Evesque

<u>Question (M. Mettenleiter)</u>
In order to guarantee the correct update of the algorithm you use a Lyapunov function. How does this function depend on the model of your combustion system?

<u>Reply</u>
The Lyapunov function is not model-based at all. Its existence relies only on the four assumptions made on our system (see paper), but no other information on the system is required in the Lyapunov stability analysis.

This page has been deliberately left blank

Page intentionnellement blanche